

The UV spectrum of the narrow-line Seyfert 1 galaxy, RE J1034+396

E. M. Puchnarewicz¹, K. O. Mason¹ and A. Siemiginowska²

¹*Mullard Space Science Laboratory, University College London, Holmbury St. Mary, Dorking, Surrey RH5 6NT, UK.*

²*Harvard-Smithsonian Center for Astrophysics, 60 Garden Street, Cambridge, MA 02138, USA.*

ABSTRACT

RE J1034+396 has one of the hottest big blue bumps of any Seyfert 1 ($kT_{\text{BB}} \sim 120$ eV) and thus provides a valuable insight into the physics in the nuclei of active galaxies. In this paper, we present UV spectroscopy of RE J1034+396, taken with the Faint Object Spectrograph on the *Hubble Space Telescope*. With a spectral resolution of $\sim 1\text{-}2$ Å FWHM and a typical signal-to-noise ratio of ~ 15 per diode, this is one of the first detailed UV spectra of an object in the narrow-line Seyfert 1 (NLS1) class. The spectrum probes the physics and kinematics of the high-ionization and coronal line gas, and the strength and form of the big blue bump component in the UV.

We detect many emission lines, including Ly α , C IV $\lambda 1549$, He II $\lambda 1640$, C III] $\lambda 1909$ and Mg II $\lambda 2798$. We also identify a feature at 2647 Å (in the rest-frame) with highly-ionized iron ([Fe XI] $\lambda 2649$); a line of the same species ([Fe XI] $\lambda 7892$) has also been seen in the optical spectrum. The velocity widths of the UV lines are relatively narrow (FWHM < 2000 km s⁻¹) although C IV $\lambda 1549$ appears to have a broad underlying component with a FWHM typical of quasars (~ 5500 km s⁻¹). The FWHM are similar to those of the optical lines, which suggests that *all* line emission in RE J1034+396, i.e. including that of high- and low-ionization species *and* the forbidden lines, may be dominated by an intermediate-velocity (FWHM ~ 1000 km s⁻¹), intermediate-density ($\log N_e \sim 7.5$ cm⁻³) region of gas. The slope of the UV continuum ($\alpha_{\text{UV}} \sim 0.9$) is soft (i.e. red) relative to quasars and the UV-to-soft X-ray flux ratio is unusually low (the 0.2 keV/1200 Å flux ratio is 1/200), implying that the big blue bump component is very weak in the UV. The present epoch UV to soft X-ray continuum is consistent with earlier data, demonstrating that this extreme big blue bump component is also very stable, unlike many other NLS1s which show extreme patterns of variability.

Key words: Galaxies: Seyfert – Galaxies: Active – X-rays: Galaxies – Accretion disks – Line: formation – Galaxies: individual: RE J1034+396.

1 INTRODUCTION

RE J1034+396 (also known as Zw 212.025) is a narrow-line Seyfert 1 galaxy (NLS1) and a rare EUV-selected AGN (Pounds et al. 1993; Mason et al. 1995). Observations of the 0.1–2.4 keV spectrum with the *ROSAT* Position Sensitive Proportional Counter (PSPC), showed that it has an unusually high temperature soft X-ray component, with a high-energy turnover at around 0.4 keV (Puchnarewicz et al. 1995; Pounds, Done & Osborne 1995). An attempt was made by Puchnarewicz et al. (1995) to measure the UV spectrum with *IUE*, but the source was found to be very faint in the UV relative to the X-rays, suggesting the lack of any big blue bump (BBB; e.g. Edelson & Malkan 1986; Elvis et al. 1994) emission down to ~ 1200 Å. This was a surprising result, considering the extreme EUV nature of the source, and suggested that the ‘big bump’ (i.e. a single component which incorporates the optical/UV BBB and the soft X-ray excess) is so hot that it is shifted out of the UV completely but dominates in the EUV and soft X-rays.

It has now been well-established that there is a strong link between the slope of the soft X-ray spectrum, α_x , and the velocity of the low-ionization line-emitting clouds in Seyfert 1s and quasars (e.g. Puchnarewicz et al. 1992; Boller, Brandt & Fink 1996; Laor et al. 1997). As a NLS1 with an ultrasoft X-ray spectrum, RE J1034+396 is entirely consistent with this behaviour, lying at one extreme of the relationship between H β FWHM and α_x .

However, very little is known of the effects, if any, of the unusual continuum shape on the high-ionization line region. Reverberation mapping models of ‘normal’ Seyfert 1s, e.g. NGC 5548 (e.g. Clavel et al. 1991; Krolik et al. 1991), suggest a large degree of stratification in the broad line region (BLR), i.e. the high-ionization lines (HILs; FWHM $\sim 5000\text{-}6000$ km s⁻¹) are produced relatively close to the black hole, while the low-ionization lines (LILs) are formed light-days to light-weeks away from the HILs (FWHM ~ 3000 km s⁻¹). A key issue in the study of NLS1s is whether the characteristics of the HILs in these objects are also related to the soft X-ray spectrum and form at rela-

tively low velocities, or whether the line-of-sight velocities of the more highly ionized line-emitting gases are independent of α_x .

Another important issue is the nature of the UV continuum itself. The lack of any BBB emission in the UV as suggested by the *IUE* data, places a very tight constraint on accretion disc (AD) models of the BBB. The softness of the optical/UV continuum and lack of any rise towards the blue, implies a very hot AD around a relatively low-mass black hole ($\sim 10^6 M_\odot$; Puchnarewicz et al. 1995). However the original *IUE* data were statistically poor, giving an unreliable flux determination and little information to constrain the UV continuum slope.

Thus to continue our investigations of the physics and geometry of RE J1034+396, we have obtained a UV spectrum with the Faint Object Spectrograph (FOS) on the *Hubble Space Telescope* (*HST*). This spectrum is a vast improvement over that obtained with *IUE*, covering a range of ~ 1200 - 3000 \AA (in the rest-frame) with a resolution of 1-2 \AA FWHM and signal to noise ratio of ~ 15 per diode. In this Letter, we report the first results from this observation.

2 OBSERVATIONS AND RESULTS

RE J1034+396 was observed by *HST* on 1997 January 31 using three gratings (G130H, G190H and G270H) covering the range 1100 \AA to 3300 \AA . All spectra were taken with the BLUE detector; details of the observations, including exposure times, are given in Table 1. The data were reduced using the standard *HST* archive pipeline processing. Errors on the observed flux in each diode are typically ~ 10 per cent in the 1100 - 1500 \AA range and 5 - 10 per cent between 1500 \AA and 3300 \AA . The flux and slope of the *HST*-FOS spectrum are consistent with the earlier *IUE* data.

Scattered light in the shortest wavelength gratings can be a problem for very red sources observed with *HST*-FOS (see e.g. the *HST*-FOS Instrument Science Reports 114 and 115). The pipeline corrects for scattered light by measuring the counts accrued in the unilluminated pixels of the array (pixels 31-130) after subtraction of the dark particle-induced current, then subtracting the mean level in this pixel range from the full G130H spectrum. The wavelength dependence of the scattered light (if any) is poorly understood however, and in some cases this first order correction is not adequate and residual scattered light remains. Examination of the raw counts and flux files for RE J1034+396 shows that the scattered light comprised at most only 20 per cent of the continuum flux at $\sim 1500 \text{ \AA}$ before correction by the pipeline, and appears to have been effectively removed. Thus no further corrections have been made to these data to account for scattered light.

The G130H/BLUE configuration has shown an increase in sensitivity of ~ 5 per cent in the 1250 to 1600 \AA range from July 1995 to late December 1996. Therefore the G130H fluxes in this range were reduced by 5 per cent to correct for this change in sensitivity. Fluxes in the 1200 \AA to 1250 \AA range were reduced by a linear ramp from 0 per cent to 5 per cent respectively.

2.1 UV emission lines

Rest-frame line positions and full widths at half maximum (FWHM) were measured from the spectrum for the

Table 1. *HST*-FOS observation log

Grating	resolution FWHM (\AA)	exp time (seconds)	range (\AA)
G130H	0.96	4420	1090-1600
G190H	1.41	2460	1580-2330
G270H	2.01	670	2230-3300

All spectra were taken through the $0.86''$ aperture and with the BLUE detector.

strongest emission lines and the results are listed in Table 2. Gaussian profile fitting was used to represent the lines while the local continuum was modelled as a second-order polynomial. Positions and FWHM of the lines are the centre and FWHM of the best-fit Gaussian profile respectively. Errors on the FWHM are difficult to determine due to problems such as continuum placement, blending with other lines, the use of multiple components in the fitting procedure and the assumption of a Gaussian profile for all components. Estimates of the errors have been made nevertheless, and were derived by comparing the data with the minima and maxima of ‘reasonable’ models, taking into account the errors on individual data points. A redshift of $z=0.043$, measured from the peak positions of the strongest emission lines, was assumed. Fits to the $\text{Ly}\alpha$, $\text{CIV}\lambda 1549$, HeII , CIII] and MgII lines are shown in Fig 1; in this figure we also indicate a line at a rest wavelength of 2647.4 \AA which has been identified with $[\text{FeXI}]\lambda 2649$. This suggests the presence of highly-ionized gas in RE J1034+396 and its implications are discussed further in Section 3.2.

In most cases (except MgII), a single Gaussian gave a poor fit to the data, so additional Gaussians were used. For $\text{Ly}\alpha$ and HeII , components from the narrow line region (NLR) were resolved with FWHM of $\sim 500 \text{ km s}^{-1}$. NLR components were not seen in $\text{CIV}\lambda 1549$, CIII] or MgII however. Although $\text{CIV}\lambda 1549$ is dominated by a feature with a FWHM of $\sim 1300 \text{ km s}^{-1}$, it appears to have a much broader (FWHM $\sim 5500 \text{ km s}^{-1}$) underlying component which contains about a third of the total line flux. Rodríguez-Pascual, Mas-Hesse & Santos-Lleó (1997) have also reported broad underlying components in the high-ionization lines of several NLS1s from *IUE* spectra, with FWHM between 5000 km s^{-1} and $10\,000 \text{ km s}^{-1}$. However, while Rodríguez-Pascual et al. (1997) find these features underlying $\text{Ly}\alpha$, $\text{CIV}\lambda 1549$ and HeII in their sample, for RE J1034+396, only the $\text{CIV}\lambda 1549$ line has a significant broad component. There is some evidence of an additional underlying component in CIII] although formally only an upper limit is obtained (FWHM $< 4300 \text{ km s}^{-1}$); the feature may instead be due to contamination by other lines or blends (see Fig 1).

2.1.1 Full widths at half maximum

The UV emission lines are all relatively narrow: the broad components of $\text{Ly}\alpha$ and HeII have FWHM of less than 2000 km s^{-1} , and MgII has a FWHM of only 1500 km s^{-1} . These FWHM are very low compared to AGN in general, for example, Brotherton et al. (1994) find mean FWHM for CIII] and MgII of 6900 km s^{-1} and 4200 km s^{-1} respectively (for their radio-quiet objects). The mean $\text{CIV}\lambda 1549$ FWHM of the radio-quiet objects from the Wills et al. (1993) sample

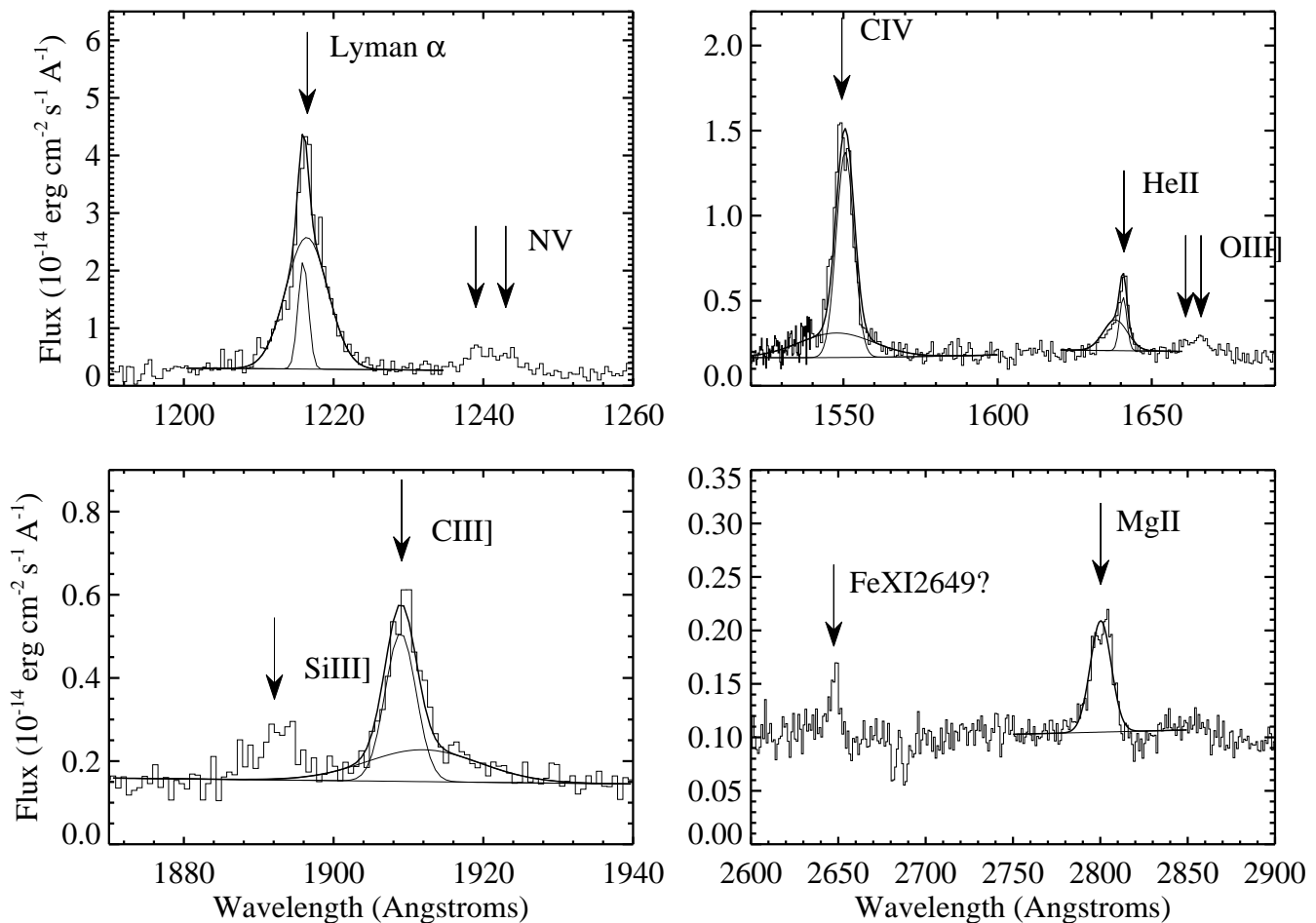


Figure 1. Gaussian fits to emission lines in the spectrum of RE J1034+396. Each portion of the spectrum has been redshifted into the rest-frame of the AGN ($z=0.043$) and the expected positions of lines commonly found in AGN spectra are indicated. The spectra have been binned by a factor of two for clarity.

is 5400 km s^{-1} , which is similar to the very broad underlying feature seen in RE J1034+396, but much broader than the FWHM of the overall profile ($\sim 1400 \text{ km s}^{-1}$).

When measured from optical spectra with a similar velocity resolution, the broad component FWHM of the Balmer lines for RE J1034+396 are also narrow (values of 1500 km s^{-1} and 1800 km s^{-1} for $H\beta$ and $H\alpha$ respectively; Puchnarewicz et al. 1995), and similar to those of the UV lines presented here. Thus low velocities in the line-emitting regions of RE J1034+396 are not confined to the Balmer lines, but are typical of low-ionization lines in the UV (e.g. MgII) and high ionization lines (e.g. Ly α and CIV λ 1549).

2.2 UV continuum slope

The slope of the continuum was measured by fitting a power-law to the data, having first removed all emission line features and regions of poor data. The best-fit was obtained for a slope, α_{uv} , of 0.9 (all indices, α , are defined such that $F_\nu \propto \nu^{-\alpha}$). This is very soft when compared to the typical UV slopes of quasars where the BBB emission is strong (e.g. Neugebauer et al. (1987) and Francis et al. (1991) find

Table 2. UV emission lines

Position Å	Identification	FWHM km s^{-1}
1216.4	Ly α (broad)	1600^{+1800}_{-200}
1216.0	Ly α (narrow)	400^{+700}_{-200}
1547.7	CIV $\lambda\lambda$ 1548,1551 (very broad)	5500^{+3000}_{-900}
1550.6	CIV $\lambda\lambda$ 1548,1551 (broad)	1300^{+500}_{-500}
1638.2	HeII (broad)	1700^{+500}_{-700}
1640.8	HeII (narrow)	500^{+200}_{-200}
1912.0	CIII] (very broad)	<4300
1909.0	CIII] (broad)	800^{+400}_{-200}
2647.4	[FeXI] λ 2649	700^{+300}_{-300}
2800.2	MgII	1500^{+400}_{-400}

median slopes of 0.2-0.3 for their quasar samples).

2.3 UV to X-ray spectrum

We have also obtained a quasi-simultaneous measurement of the strength of the soft X-ray spectrum with the High Reso-

lution Imager (HRI; David et al. 1996) on *ROSAT* (Trumper 1983). These data were taken on 1996 November 12 and yield a count rate of 0.61 ± 0.02 count sec^{-1} . This is consistent with the earlier *ROSAT*-PSPC spectrum taken 1991 November (Puchnarewicz et al. 1995).

A spectrum of RE J1034+396 from the UV to X-rays (3000 Å to 2 keV) is shown in Figure 2. This spectrum combines the *HST*-FOS data with the model fitted to the *ROSAT*-PSPC spectrum (from Puchnarewicz et al. 1995) which has been normalized to the HRI count rate. Assuming isotropic emission from the UV to soft X-rays, we measure a luminosity from 3000 Å to 2 keV of 3×10^{44} erg s^{-1} (the Hubble constant, $H_0 = 75$ km s^{-1} Mpc $^{-1}$ and deceleration parameter, $q_0 = 0$; the unobserved 1200 Å to 0.1 keV part of the spectrum was interpolated linearly from the observed data). The 0.1 to 2 keV spectrum dominates the luminosity overall in this range, with $L = 2 \times 10^{44}$ erg s^{-1} .

The figure shows the unusually high ratio of soft X-ray to UV flux; the ratio of the 0.2 keV to 1200 Å fluxes is ~ 200 , whereas for AGN in general, this ratio is usually less than 1. In addition, there is no sign of any steep rise in the UV continuum towards the EUV which is required to meet the soft X-ray data. It suggests that the relative contribution of the big bump, even at ~ 1200 Å, is very weak.

Reddening by dust is unlikely to be the cause of the weak UV flux. The UV continuum doesn't turn down towards the blue as would be expected ($\alpha_{\text{uv}} = 0.9$; Section 2.2) and there is no sign of the broad 2200 Å dust absorption feature. In the optical, the Balmer decrement is relatively low (~ 3 ; Puchnarewicz et al. 1995) while the strong soft X-ray spectrum, which shows no evidence for warm absorber edges, implies that columns of accompanying cold or warm gas must be low.

3 DISCUSSION

RE J1034+396 is one of only a handful of AGN which have been selected by the strength of its EUV emission. It has a very hot BBB (Puchnarewicz et al. 1995) and a very soft 2-10 keV power-law continuum slope ($\alpha = 1.6$; Pounds et al. 1995). Both its permitted and forbidden optical emission lines appear to be dominated by a line region which is 'intermediate' in terms of its velocity, and perhaps also in its density and position relative to the typical broad and narrow line regions (Mason et al. 1996).

With these *HST* data, we have probed further into the emission line regions of RE J1034+396, investigating the production of the high-ionization lines which, in some systems, are thought to be produced closer to the central black hole. We have also measured the shape and strength of the UV continuum, and searched for a rise in the slope which would indicate the emerging low energy tail of the big bump and constrain accretion disc models.

3.1 High-temperature big bump

The lack of any significant big bump emission in the UV combined with the high energy turnover in soft X-rays define a high-temperature extreme for current models of this component. The data presented here (*HST* plus HRI) are consistent with the earlier *IUE* plus PSPC spectra, demonstrating a remarkable degree of stability for RE J1034+396,

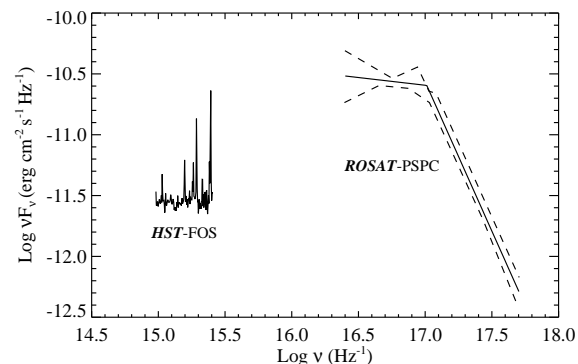


Figure 2. The UV to X-ray spectrum of RE J1034+396 (shown as a solid line), combining the *HST*-FOS and *ROSAT*-PSPC data (normalized to the HRI flux), and plotted in the rest-frame of the AGN. The dashed lines indicate 90 per cent errors on the broken power-law fit to the *ROSAT*-PSPC data.

especially when considered with other objects in the NLS1 class which have shown extreme changes on long and short timescales. For example, RE J1237+264 changed by a factor of 70 in 18 months; Brandt, Pounds & Fink 1995), while the soft X-ray flux of IRAS 13224-3809 has been observed to double in only 800 sec (Boller et al. 1993).

The apparent lack of variability in the UV to X-ray spectrum of RE J1034+396 can also provide a useful discriminant for models of the big bump. Pounds et al. (1995) have suggested that RE J1034+396 may be a supermassive analogue of a galactic black hole candidate (GBHC) in a high state, where the system is accreting close to its Eddington limit. In this state, the X-ray spectrum has a steep soft component which is relatively stable, and a weak power-law tail extending to higher energies which is highly variable (see e.g. Tanaka & Lewin 1995). RE J1034+396 has a stable ultrasoft component and, although Puchnarewicz et al. (1995) showed that a sub-Eddington accretion rate is consistent with the observed UV to X-ray continuum, these AD models are poorly constrained and even super-Eddington discs cannot be ruled out. RE J1034+396 also has a weak power-law tail like a high-state GBHC, although there was no evidence of significant flux or spectral variability during the *ASCA* 1-10 keV observation (Pounds et al. 1995), which contradicts the GBHC analogy.

3.2 Emission line regions

As well as measurements of the UV continuum flux and slope, these *HST* data have revealed a wealth of emission lines, including Ly α , C IV $\lambda 1549$, He II, C III and Mg II (see Fig. 1 and Table 2). We also detect [Fe I] $\lambda 2649$; the [Fe I] $\lambda 7892$ line, a different transition within the same ionization species, has also been observed in the optical/IR (Puchnarewicz et al. 1995). These lines indicate the presence of highly ionized gas in RE J1034+396 and, based on theoretical ratios given by Penston et al. (1984), the observed [Fe I] $\lambda 2649$ /[Fe I] $\lambda 7892$ flux ratio of ~ 0.4 suggests emission from a photoionized gas at a temperature of $\sim 4 \times 10^4$ K or collisionally-ionized gas with $T \sim 10^6$ K. The observed ratio was calculated using the [Fe I] $\lambda 7892$ data from Puchnarewicz et al. (1992) and an [Fe I] $\lambda 2649$ flux of

4×10^{-15} erg cm $^{-2}$ s $^{-1}$ Å $^{-1}$ measured from the FOS data.

The composite UV line profiles are all unusually narrow with FWHM of $\lesssim 2000$ km s $^{-1}$. These are similar to the FWHM of the Balmer lines in RE J1034+396 measured from low-resolution optical spectra. In the case of the Balmer lines, subsequent high-resolution data showed that the profiles were dominated by an ‘intermediate’ velocity component (FWHM ~ 1000 km s $^{-1}$; Mason et al. 1996). This intermediate component was also seen in the forbidden lines, suggesting that the region which produced much of the Balmer line and forbidden line emission was intermediate in terms of its density *and* velocity. Thus it is possible that this same intermediate velocity component dominates the HILs as well, implying that one region produces the bulk of the HIL, LIL *and* the forbidden line emission in RE J1034+396. This is in contrast to models of more typical Seyfert 1s developed from reverberation mapping analyses (e.g. Krolik et al. 1991), where the HIL region lies close to the black hole and has relatively high velocity, whereas the LIL region lies ~ 10 -100 light-days away and has relatively low velocity.

The high-resolution optical data also revealed the presence of a broad underlying component (i.e. FWHM of ~ 2500 km s $^{-1}$), suggesting that a ‘normal’ Balmer line region does exist in RE J1034+396, albeit weak. In these FOS data, again while a low-velocity component dominates in the HIL profiles, C IV $\lambda 1549$ does have a very broad underlying component (FWHM ~ 5500 km s $^{-1}$), typical of quasars in general. This suggests the presence of a ‘normal’ HIL region as well, although again this is weak relative to the lower-velocity gas.

The apparent difference in BLR geometry between narrow-line and ordinary Seyfert 1s may be due to a fine-tuning of the conditions necessary for efficient line production. Baldwin et al. (1995) suggested that line emission is strongest where the combination of input ionizing continuum and gas density are optimized for that particular line species. In the case of RE J1034+396 (and perhaps all NLS1s), this may be at distances relatively far out from the centre, because either: 1. there is very little line-emitting gas closer to the nucleus; or 2. the extreme softness of the ionizing continuum tends to produce most of the line emission at greater distances where the density is lower.

4 SUMMARY

We have presented the UV spectrum of RE J1034+396 in the 1200-3100 Å range, and supporting quasi-simultaneous soft X-ray data from the ROSAT HRI. These data confirm the existence of a very hot big bump component in RE J1034+396, whose emission is *not* significant in the UV. The big bump appears to have been stable over a period of five years, which is remarkable for a NLS1 since many objects in this class have shown extreme variability in the UV and soft X-rays. The FWHM of the high ionization lines are narrow ($\lesssim 2000$ km s $^{-1}$) and similar to those of the low ionization lines (including Mg II and the Balmer lines). With the apparent dominance of an intermediate velocity component in both the Balmer lines and [O III] $\lambda\lambda 4959, 5007$, this suggests that *all* types of line emission in RE J1034+396, i.e. HILs, LILs and forbidden lines, may be dominated by the same region of gas. This geometry contrasts sharply with that derived for normal Seyfert 1s, where the BLR is highly

stratified and the HIL and LIL regions are separated by ~ 10 -100 light-days. The presence of [Fe X] $\lambda 2649$ in the UV spectrum indicates the presence of highly-ionized gas in the system, which may be collisionally-ionized or photoionized.

ACKNOWLEDGEMENTS

We thank Martin Ward and the referee, Niel Brandt, for their comments and advice. This work was supported by HST grant GO-06600.01-95A and NASA contract NAS8-39073.

REFERENCES

- Baldwin J. A., Ferland G., Korista K., Verner D., 1995, ApJ, 455, L119
 Baldwin J. A., Wampler E. J., Gaskell C. M., 1989, ApJ, 338, 630
 Boller Th., Brandt W. N., Fink H., 1996, A&A, 305, 53
 Boller T., Truemper J., Molendi S., Fink H., Schaeidt S., Caulet, A., Dennefeld M., 1993, A&A, 279, 53
 Brandt W. N., Pounds K. A., Fink H., 1995, MNRAS, 273, L47
 Brotherton M. S., Wills B. J., Steidel C. C., Sargent W. L. W., 1994, ApJ, 423, 131
 Clavel J. et al., 1991, ApJ, 366, 64
 David L. P., Harnden F. R., Kearns K. E., Zombeck M. V., 1996, in ‘The ROSAT High Resolution Imager’, SAO Press, Cambridge
 Edelson R. A., Malkan M. A., 1986, ApJ, 308, 509
 Elvis M., Wilkes B., M^cDowell J. C., Green R. F., Bechtold J., Willner S. P., Oey M. S., Polowski E., Cutri R., 1994, ApJS, 95, 1
 Francis P. J., Hewett P. C., Foltz C. B., Chaffee F. H., Weymann R. J., Morris S. L., 1991, ApJ, 373, 465
 Krolik J. H., Horne K., Kallman T. R., Malkan M. A., Edelson R. A., Kriss G. A., 1991, ApJ, 371, 541
 Laor A., Fiore F., Elvis, M., Wilkes, B. J., M^cDowell, J. C., 1997, ApJ, 477, 93
 Malkan M. A., 1984, in *X-ray and UV Emission from Active Galactic Nuclei*, ed. W. Brinckmann and S. Trumper (MPIfR), 121
 Mason K. O. et al., 1995, MNRAS, 274, 1194
 Mason K. O., Puchnarewicz E. M., Jones L. R., 1996, MNRAS, 283, L26
 Neugebauer G., Green R. F., Matthews K., Schmidt M., Soifer B. T., Bennet J., 1987, ApJS, 63, 615
 Penston M. V., Fosbury R. A. E., Boksenberg A., Ward M. J., Wilson A. S., 1984, MNRAS, 208, 347
 Pfeffermann E. et al., 1986, Proc. S. P. I. E., 733, 519
 Pounds K. A. et al., 1993, MNRAS, 260, 77
 Pounds K. A., Done C., Osborne J. A., 1995, MNRAS, 277, L5
 Puchnarewicz E. M., Mason K. O., Córdova F. A., Kartje J., Branduardi-Raymont G., Mittaz J. P. D., Murdin P. G., Allington-Smith J., 1992, MNRAS, 256, 589
 Puchnarewicz E. M., Mason K. O., Siemiginowska A., Pounds K. A., 1995, MNRAS, 276, 20
 Rodríguez-Pascual P., Mas-Hesse J. M., Santos-Lleó M., 1997, A&A, 1997, in press
 Tanaka Y., Lewin W. H. G., 1995, in ‘X-ray Binaries’, ed. W. H. G. Lewin, J. van Paradijs & E. P. J. van den Heuvel (Cambridge: Cambridge University Press), p252
 Trumper J., 1983, Adv. Space Res., 4, 241
 Wells A. A. et al., 1990, Proc. S. P. I. E., 1344, 230
 Wills B. J., Brotherton M. S., Fang D., Steidel C. C., Sargent W. L. W., 1993, ApJ, 415, 563

This paper has been produced using the Royal Astronomical Society/Blackwell Science T_EX macros.